

An X-ray Absorption Spectroscopic Structural Investigation of the Nickel Site in *Escherichia coli* NikA Protein

Christian B. Allan,[†] Long-Fei Wu,[‡] Zhijie Gu,[†]
 Suranjan B. Choudhury,[†] Faizah Al-Mjeni,[†]
 Manju L. Sharma,[†]
 Marie-Andrée Mandrand-Berthelot,[‡] and
 Michael J. Maroney^{*,†}

Department of Chemistry, University of Massachusetts, Amherst, Massachusetts 01003-4510, and Laboratoire de Génétique Moléculaire des Microorganismes, CNRS-URA 1486, INSA, 69621 Villeurbanne Cedex, France

Received April 9, 1998

Since the discovery of the involvement of Ni in the active site of the enzyme urease in 1975,¹ the role of Ni in biology has been rapidly expanding. The list of nickel-dependent metalloenzymes now includes acetyl coenzyme A synthase/carbon monoxide dehydrogenase,^{2–4} methyl coenzyme M reductase,^{5,6} Ni/Fe hydrogenases,^{7,8} and superoxide dismutases from *Streptomyces*.^{9,10} Each of these enzymes appears to be dependent on several gene products that constitute a Ni-specific transport and metalcenter assembly system.¹¹ We report here the results of an X-ray spectroscopic structural investigation of the Ni site in a Ni transport protein, the periplasmic Ni-binding protein, NikA, from *Escherichia coli*.

NikA is the protein encoded by the *nikA* gene, which is part of the five-gene (*nikA–E*) *nik* operon of *E. coli* that encodes a high-affinity nickel-specific transport system.¹² The first gene, *nikA*, encodes a protein with a molecular weight of 56 kDa that specifically binds a single Ni²⁺ ion with high affinity ($k_d \approx 0.1 \mu\text{M}$).¹³ The only known nickel-containing enzymes in *E. coli* are three hydrogenase isoenzymes, which are expressed under anaerobic growth conditions and require the Nik proteins for

activity.^{14,15} In addition to its role in making Ni available for the biosynthesis of hydrogenases, NikA also serves in the Tar-dependent negative chemotaxis associated with higher concentrations of Ni²⁺, which are toxic to both eukaryotic and prokaryotic organisms.¹⁶

Experimental Section

Protein Production and Purification. A sample of NikA was prepared as previously described.¹³ The periplasmic nickel-binding protein NikA was overproduced by cloning the *nikA* gene into an overexpression vector, pRE1, and purified to near homogeneity by hydrophobic and ion-exchange chromatography.

Synthesis of Ni(sal)₂(H₂O)₂. This compound was synthesized according to published procedures.¹⁷ The crystal structure of this model complex reveals a pseudo-octahedral, NiO₆ site, composed of four O donors from salicylate and two O donors from axial water molecules, with an average Ni–O bond length of 2.03(1) Å.¹⁸

X-ray Absorption Spectra (XAS) Data Collection and Analysis. Ni K-edge XAS data were collected on beamline X9B at the National Synchrotron Light Source at Brookhaven National Laboratory. Data were collected under dedicated conditions at ca. 2.5 GeV and 100–220 mA with a 1-mm vertical hutch aperture. A Si[111] crystal monochromator was used for XAS data collection for the NikA protein (0.5 mM) and a Si[220] crystal monochromator for the Ni(sal)₂(H₂O)₂ model complex. The monochromators were internally calibrated to the first inflection point of Ni foil (8331.6 eV). These arrangements provided a theoretical resolution of ca. 1–2 eV for the protein and 0.5–1 eV for the model compound. The precision of the edge energy calibrations is ~ 0.2 eV. Harmonic rejection was accomplished with use of a focusing mirror left flat at an angle of 4.5°. Fluorescence data were collected on two frozen solutions of the NikA protein at 60 K with use of a He displacer unit and a 13-element Ge detector (Canberra). Sample integrity was judged by examining the edge region as a function of exposure time and by examining the CD spectrum of the transport protein before and after exposure to synchrotron radiation. Neither spectrum revealed any changes in the sample after it was exposed. Spectra from two samples were measured on separate runs, and the results from the two data sets agree. Model compound data were collected at 60 K in transmission mode on powdered samples dispersed on layers of Kapton tape.

The analysis of the XAS data was carried out according to procedures previously described in detail.^{19,20} Data over the range of $k = 2.0–12.5 \text{ \AA}^{-1}$ were used to generate a Fourier transformed spectrum. Fourier filtered extended X-ray absorption fine structure (EXAFS) data sets were generated using backtransform windows with $r = 1.1–2.0$ or $1.1–2.6 \text{ \AA}$ (uncorrected for phase shifts). The EXAFS data were corrected for detector efficiencies, absorbance by air and cryostat windows, and the variation with energy of the sample X-ray penetration depth.²¹ Least-squares fits of the data following a protocol that restricts the number of scattering atoms to integer values were performed using single-

* Corresponding author at Lederle Graduate Research Center, Department of Chemistry, University of Massachusetts, P.O. Box 34510, Amherst, MA 01003-4510. Phone: 413-545-4876. Fax: 413-545-4490. E-mail: MMaroney@Chem.UMass.edu.

[†] Department of Chemistry.

[‡] Laboratoire de Génétique Moléculaire des Microorganismes.

- (1) Dixon, N. E.; Gazzola, C.; Blakeley, R. L.; Zerner, B. *J. Am. Chem. Soc.* **1975**, *97*, 4131–4133.
- (2) Ferry, J. G. *Annu. Rev. Microbiol.* **1995**, *49*, 305–333.
- (3) Tan, G. O.; Ensign, S. A.; Ciurli, S.; Scott, M. J.; Hedman, B.; Holm, R. H.; Ludden, P. W.; Korszun, Z. R.; Stephens, P. J.; Hodgson, K. O. *Proc. Natl. Acad. Sci. U.S.A.* **1992**, *89*, 4427–4431.
- (4) Xia, J.; Dong, J.; Wang, S.; Scott, R. A.; Lindahl, P. A. *J. Am. Chem. Soc.* **1995**, *117*, 7065–7070.
- (5) Jaun, B. *Chimia* **1994**, *48*, 50–55.
- (6) Ermler, U.; Grabarse, W.; Shima, S.; Goubeaud, M.; Thauer, R. K. *Science* **1997**, *278*, 1457–1462.
- (7) Albracht, S. P. J. *Biochim. Biophys. Acta* **1994**, *1188*, 167–204.
- (8) Volbeda, A.; Garcin, E.; Piras, C.; de Lacey, A. L.; Fernandez, V. M.; Hatchikian, E. C.; Frey, M.; Fontecilla-Camps, J. C. *J. Am. Chem. Soc.* **1996**, *118*, 12989–12996.
- (9) Youn, H.-D.; Youn, H.; Lee, J.-W.; Yim, Y.-I.; Lee, J. K.; Hah, Y. C.; Kang, S.-O. *Arch. Biochem. Biophys.* **1996**, *334*, 341–348.
- (10) Youn, H.-D.; Kim, E.-J.; Roe, J.-H.; Hah, Y. C.; Kang, S.-O. *Biochem. J.* **1996**, *318*, 889–896.
- (11) Hausinger, R. P. J. *Biol. Inorg. Chem.* **1997**, *2*, 279–286.
- (12) Navarro, C.; Wu, L.-F.; Mandrand-Berthelot, M.-A. *Mol. Microbiol.* **1993**, *9*, 1181–1191.
- (13) De Pina, K.; Navarro, C.; McWalter, L.; Boxer, D. H.; Price, N. C.; Kelly, S. M.; Mandrand-Berthelot, M.-A.; Wu, L.-F. *Eur. J. Biochem.* **1995**, *227*, 857–865.

- (14) Sawers, R. G.; Ballantine, S. P.; Boxer, D. H. *J. Bacteriol.* **1985**, *164*, 1324–31.
- (15) Wu, L. F.; Mandrand, M. A. *FEMS Microbiol. Rev.* **1993**, *104*, 243–269.
- (16) Charon, M.-H.; Wu, L.-F.; Piras, C.; de Pina, K.; Mandrand-Berthelot, M.-A.; Fontecilla-Camps, J. C. *J. Mol. Biol.* **1994**, *243*, 353–355.
- (17) Tyson, G. N., Jr.; Adams, S. C. *J. Am. Chem. Soc.* **1940**, *62*, 1228–1229.
- (18) Stewart, J. M.; Lingafelter, E. C.; Breazeale, J. D. *Acta Crystallogr.* **1961**, *14*, 888–891.
- (19) Bagyinka, C.; Whitehead, J. P.; Maroney, M. J. *J. Am. Chem. Soc.* **1993**, *115*, 3576–3585.
- (20) Colpas, G. J.; Maroney, M. J.; Bagyinka, C.; Kumar, M.; Willis, W. S.; Suib, S. L.; Mascharak, P. K.; Baidya, N. *Inorg. Chem.* **1991**, *30*, 920–928.
- (21) Scarrow, R. C.; Maroney, M. J.; Palmer, S. M.; Que, L., Jr.; Roe, A. L.; Salowe, S. P.; Stubbe, J. *J. Am. Chem. Soc.* **1987**, *109*, 7857–7864.

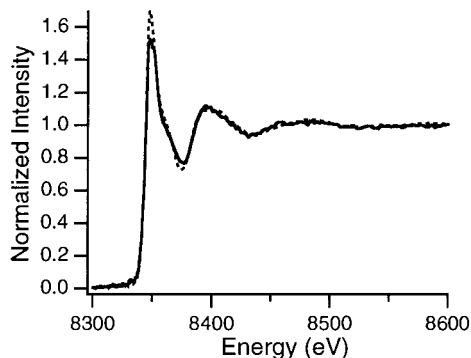


Figure 1. Ni K-edge XAS spectra in the edge and XANES region for Nika (solid line) and for Ni(sal)₂(H₂O)₂ (dashed line).

scattering EXAFS theory as previously described.²² Empirical parameters used in generating the fits were obtained from Ni(sal)₂(H₂O)₂ ($A = 0.46$, $\Delta E = 4.86$ eV, and $\sigma^2 = 0.002$). Best fits were judged by minimizing the goodness-of-fit criterion ($GOF = \{n(\text{idp})/[n(\text{idp}) - n(\text{p})]\}^{1/2} R$, where $R = \text{av}[(\text{data simulation})/\text{estimated standard deviation of data}]$, $n(\text{p})$ = the number of varied parameters, and $n(\text{idp})$ = the number of data points for unfiltered refinements or $2(r_{\text{max}} - r_{\text{min}})(k_{\text{max}} - k_{\text{min}})/\pi$ for filtered refinements) and the difference in the disorder between model compounds and the fit [$\Delta\sigma^2 = |\sigma_{\text{m}}^2 - \sigma_{\text{model}}^2|$] using single-scattering EXAFS theory.

The area under the XANES features assigned to $1s \rightarrow 3d$ transitions found in the preedge region at about 8332 eV was determined for each sample after background correction. These areas are useful in determining the geometry and coordination number of the Ni site.²⁰ For purposes of comparison, the edge energies reported are taken to be the energy at a normalized intensity of 0.5.

Results and Discussion

Ni K-Edge and XANES Studies. Figure 1 shows the normalized Ni K-edge XAS spectra in the edge and XANES regions obtained from Nika and a model complex used for comparison, Ni(sal)₂(H₂O)₂. The edge energy for the Nika spectrum is 8342.5(2) eV, typical of a Ni(II) complex with hard (i.e., O or N) donor ligands. Within our ability to measure it, this edge energy is identical to that obtained for Ni(sal)₂(H₂O)₂ [8342.5(2) eV], which indicates that the charge density residing on the Ni center is identical in the two complexes.²⁰ The assignment of an oxidation state of Ni(II) in Nika is also consistent with the lack of an electron paramagnetic resonance signal from the sample^{23,24} and with the descriptive chemistry of Ni.^{25,26}

The absence of a preedge peak at around 8338 eV that is assigned to a $1s \rightarrow 4p_z$ transition (with shake-down contributions) in planar 4-coordinate Ni complexes demonstrates that the Ni site in Nika is not planar.²⁰ There is a weak peak near 8333 eV in the spectrum of Nika that is assigned to a symmetry-forbidden $1s \rightarrow 3d$ electronic transition. The area under this peak [$3.6(5) \times 10^{-2}$ eV] is indicative of a more centrosymmetric complex and lies in the range that is typical of 6-coordinate Ni complexes,²⁰ including Ni(sal)₂(H₂O)₂ [$2.0(5) \times 10^{-2}$ eV]. The preedge analysis is thus consistent with a 6-coordinate Ni site.²⁰ In addition to the similarities in the edge energy and preedge XANES features, the spectra obtained for Nika and for Ni-

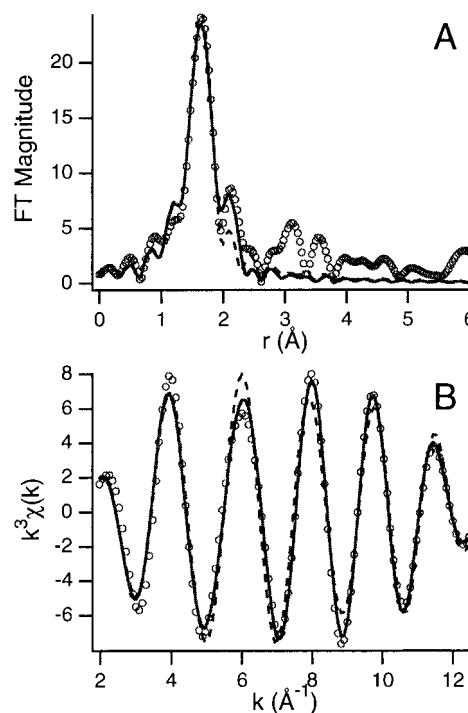


Figure 2. Ni K-edge EXAFS spectra for Nika. (A) Fourier transformed spectra (open circles) and fits. (B) Fourier filtered data using a backtransform window = 1.1–2.6 Å (open circles) and fits. The fits shown are for 6 O at 2.06(2) Å (dashed line) and for 6 O at 2.06(2) Å + 1 S at 2.57(2) Å (solid line).

Table 1. Selected Fits to Filtered Ni K-edge EXAFS Data for Nika (Backtransform Windows = 1.1–2.0 and 1.1–2.6 Å)^a

no. of shells	N	r (Å)	σ^2 ($\times 10^3$ Å ²)	$\Delta\sigma^2$ ($\times 10^3$ Å ²)	GOF
1.1–2.0 Å					
1	6	Ni–O = 2.056(1)	0.8(1)	–1.4	0.47
1	7	Ni–O = 2.056(1)	1.2(2)	–1.0	0.75
1.1–2.6 Å					
1	7	Ni–O = 2.057(2)	1.8(2)	–0.4	1.24
1	8	Ni–O = 2.057(2)	2.8(3)	0.6	1.47
2	1	Ni–S = 2.561(6)	1.9(7)	–1.3	0.88
	7	Ni–O = 2.056(1)	1.8(2)	–0.4	
2	1	Ni–S = 2.568(1)	2.0(7)	–1.2	0.78
	6	Ni–O = 2.056(6)	0.7(1)	–1.5	
2	2	Ni–S = 2.561(7)	7.7(9)	4.5	0.90
	6	Ni–O = 2.057(1)	0.7(2)	–1.5	

^a Fourier transform limits are $k = 2.0\text{--}12.5$ Å^{–1}; backtransform limits are uncorrected for phase shifts. σ^2 is the root-mean-square disorder in the Ni–L distances; $\Delta\sigma^2$ is the difference between the σ^2 value measured for the enzyme and the value determined for the reference compound; GOF is the goodness-of-fit defined in the Experimental Section. Best fits are selected to reflect the best combination of low GOF values and acceptable values of σ^2 . For the best fits shown, no parameters were correlated with a correlation coefficient > 0.6.

(sal)₂(H₂O)₂ are strikingly similar in terms of their postedge XANES features, which indicates a strong similarity between the model and the Ni site in Nika. These similarities include the white-line intensity [the most intense feature in the normalized spectrum (1.5 for Nika and 1.7 for the model)] that is consistent in both cases with a Ni environment composed of 6 O- or N-donor ligands.²⁰

Ni EXAFS Spectra. The analysis of the EXAFS data obtained for Nika is summarized in Figure 2 and Table 1. The Fourier transformed spectrum shown in Figure 2A features two peaks near 2 Å, suggesting that there are two widely differing Ni-ligand distances. When the data were filtered using a

(22) Maroney, M. J.; Colpas, G. J.; Bagyinka, C.; Baidya, N.; Mascharak, P. K. *J. Am. Chem. Soc.* **1991**, *113*, 3962–3972.

(23) Salerno, J. C. In *The Bioinorganic Chemistry of Nickel*; Lancaster, J. R., Jr., Ed.; VCH: New York, 1988; Chapter 3.

(24) Lappin, A. G.; McAuley, A. *Adv. Inorg. Chem.* **1988**, *32*, 241–294.

(25) Greenwood, N. N.; Earnshaw, A. *Chemistry of the Elements*; Pergamon Press: New York, 1984; pp 1333–1335.

(26) Cotton, F. A.; Wilkinson, G. In *Advanced Inorganic Chemistry*, 5th ed.; John Wiley and Sons: New York, 1988; p 741.

backtransform window of 1.1–2.0 Å (without correction for phase shifts), the best fit consists of 6(1) O(N) donors at a distance of 2.06(2) Å. If the second peak is included in the backtransform (1.1–2.6 Å), a second shell-scattering atom greatly improves the fit relative to a single shell of 7 O donors. Fits employing a second shell of low-*Z* scattering atoms did not improve the fit; however, addition of a long S(Cl) or first-row transition metal (e.g., Ni) leads to an improvement in the fit. The fit obtained by adding a single S donor at 2.57(2) Å to 6 O donors at 2.06(2) Å is the best fit to the data.

Although EXAFS cannot generally distinguish between O- and N-donor ligands, fits obtained by using O parameters consistently gave better results. This observation is consistent with the bond lengths obtained from the analysis [2.06(2) Å], which are indistinguishable from those found in the model compound [2.03(1) Å] and shorter than the Ni–N distances found in [Ni(Im)₆](BF₄)₂ [2.12(1) Å].²⁷ The Ni–O(N) distances found, therefore, suggest that the Ni site in NikA is dominated by O-donor ligands. There is little evidence in the EXAFS spectra of scattering arising from second and third coordination sphere C(N) atoms that would be expected if the coordination environment of the Ni center were dominated by histidine imidazole coordination. Nonetheless, the possible involvement of one or two histidine ligands cannot be ruled out entirely on the basis of the average Ni–O or N–N distances or by the absence of the characteristic spectral features.

The dominant role of O-donor ligands in the NikA Ni site is also consistent with the amino acid content of the protein.^{12,13} From a total of 502 amino acids in the mature NikA protein, 57 are aspartic and glutamic acid residues (12% of the amino acid content), and 19 are tyrosine residues, but only 10 histidine and 10 methionine and no cysteine residues are found. The Ni–O(N) distance found for NikA is also in agreement with known Ni–O_{carboxylate} distances in 6-coordinate model compounds (for example, in diaquobis(methoxyacetato)Ni(II), Ni–O_{carboxylate} = 2.05(1) Å²⁸).

The distance found for the S-donor ligand [2.57(2) Å] is similar to Ni–S distances found in 6-coordinate Ni(II) complexes, which range from 2.39 to 2.53 Å in the few structurally characterized examples.^{29–33} Among these examples are complexes with either thioether or thiolate ligands; thus, it is difficult to distinguish methionine from cysteine coordination on the basis of the Ni–S distance found. However in this case, there are no cysteine residues in the mature protein. The only cysteine residue present in the predicted amino acid sequence is lost upon cleavage of a 22 amino acid signal peptide.¹³ Thus, if this feature is attributed to an S-donor ligand, it must be a methionine ligand.

Although better fits are obtained for 1 or 2 S(Cl) donors rather than for a second Ni atom, it is often difficult to discriminate between long-S coordination and the presence of a metal center at a comparable distance (particularly when the specific metal involved is not known).³⁴ Furthermore, the 2.4-Å bond distance found when Ni is used in place of S is fairly typical of the M–M distances in many dinuclear metal sites.

The inclusion of the long-S scattering atom brings the total number of ligand donor atoms to about 7. The exact number of ligand donor atoms is poorly determined by EXAFS analysis, largely because of correlations between the number of scattering atoms and the disorder parameter, σ^2 , with the usual error in the number of identical scattering atoms being ca. $\pm 25\%$, or 1 atom in 4. Thus, the EXAFS analysis of the NikA Ni site is also consistent with 5–7 O(N)-donor and 1 S(Cl)-donor ligands. However, the values of $\Delta\sigma^2$ for O are always negative for fewer than 8 O atoms, suggesting that the number of O atoms used in the best fit (6) might be too small. Furthermore, it is easy to understand how a low coordination number can be obtained in a disordered ligand environment, but it is more difficult to rationalize a coordination number that is consistently >6 . A coordination number of 7 is unusual but not unprecedented for Ni(II). The known examples are all pentagonal-bipyramidal complexes formed between pentadentate O- or N-donor macrocyclic ligands in an equatorial plane and two axial solvent molecules.³⁵ The high percentage of carboxylate donors in NikA suggests that the first coordination sphere may be dominated by carboxylate oxygen atoms. These carboxylate ligands may be either monodentate or bidentate, a feature that may help to account for the higher coordination number indicated by the EXAFS analysis.

The results of the XAS structural investigation of the Ni site in NikA allow the Ni-ligand environment to be compared with those found in other Ni-binding proteins and Ni sites in enzymes. Through the use of molecular biological techniques, gene products that are involved in Ni-specific transport and metal-locenter assembly have been found in many organisms that utilize nickel. In addition to the NikA–E proteins, these gene products include HoxN in *Alcaligenes eutrophus*,³⁶ HupN–P in *Bradyrhizobium japonicum*,³⁷ and UreD–G in *Klebsiella aerogenes*.³⁸ UreE is the only other Ni site that has been structurally characterized in a Ni-binding protein that is involved in the transport or incorporation of Ni into an enzyme.³⁹ This protein is 1 of 4 (UreD–G) that is required for the assembly of the urease dinickel active site. In contrast to NikA, which binds a single Ni ion, UreE is a dimeric cytoplasmic protein that binds ~ 6 Ni ions. XAS studies of UreE demonstrate that the *average* environment of the 6 Ni centers in the protein is 6-coordinate and composed of O(N)-donor ligands, similar to that found for NikA. However in UreE, the ligand environment is dominated by histidine coordination, with an average of 4 ± 1 histidine ligands per Ni center.

The Ni-coordination environment in NikA is also generally similar to those found in nonredox, hydrolytic enzymes (i.e., ureases^{40,41}) and distinct from the Ni sites typical of redox enzymes (e.g., hydrogenases,⁸ methyl coenzyme M reductase⁶). Many XAS studies of Ni metalloenzymes^{3,4,19,42–46} have contributed to the characterization of the Ni-ligand environments in these enzymes. In general, the Ni sites in the redox enzymes are dominated by cysteine ligation whereas the Ni sites in

(27) van Ingen Schenau, A. D. *Acta Crystallogr. B* **1975**, *31*, 2736–2738.

(28) Prout, C. K.; Walker, C.; Rossotti, F. J. C. *J. Chem. Soc. A* **1971**, 556–558.

(29) Osakada, K.; Yamamoto, T.; Yamamoto, A.; Takenaka, A.; Sasada, Y. *Acta Crystallogr. C* **1984**, *40*, 85–87.

(30) Yamamoto, T.; Sekine, Y. *Inorg. Chim. Acta* **1984**, *83*, 47–53.

(31) Rosenfield, S. G.; Berends, H. P.; Gelmini, L.; Stephan, D. W.; Mascharak, P. K. *Inorg. Chem.* **1987**, *26*, 2792–2797.

(32) Krüger, H.-J.; Holm, R. H. *J. Am. Chem. Soc.* **1990**, *112*, 2955–2963.

(33) Setzer, W. N.; Ogle, C. A.; Wilson, G. S.; Glass, R. S. *Inorg. Chem.* **1983**, *22*, 266–271.

(34) Gu, Z.; Dong, J.; Allan, C. B.; Choudhury, S. B.; Franco, R.; Moura, J. J. G.; Moura, I.; LeGall, J.; Przybyla, A. E., et al. *J. Am. Chem. Soc.* **1996**, *118*, 11155–11165.

(35) Melnik, M.; Sramko, T.; Dunaj-Jurco, D.; Sirota, A.; Holloway, C. E. *Rev. Inorg. Chem.* **1994**, *14*, 2–346.

(36) Wolfram, L.; Friedrich, B.; Eitinger, T. *J. Bacteriol.* **1995**, *177*, 1840–3.

(37) Fu, C.; Javedan, S.; Moshiri, F.; Maier, R. J. *Proc. Natl. Acad. Sci. U.S.A.* **1994**, *91*, 5099–5103.

(38) Lee, M. H.; Mulrooney, S. B.; Renner, M. J.; Markowicz, Y.; Hausinger, R. P. *J. Bacteriol.* **1992**, *174*, 4324–4330.

(39) Lee, M. H.; Pankratz, H. S.; Wang, S.; Scott, R. A.; Finnegan, M. G.; Johnson, M. K.; Ippolito, J. A.; Christianson, D. W.; Hausinger, R. P. *Protein Sci.* **1993**, *2*, 1042–1052.

urease, NikA, and UreE are dominated by O(N)-donor ligands. Thus, the trend is for biological redox-active Ni centers to be closely associated with thiolate ligation whereas those with nonredox roles lack Ni–thiolate bonds.

-
- (40) Jabri, E.; Karplus, P. A. *Biochemistry* **1996**, *35*, 10616–10626.
(41) Karplus, P. A.; Pearson, M.; Hausinger, R. P. *Acc. Chem. Res.* **1997**, *30*, 330–337.
(42) Whitehead, J. P.; Gurbiel, R. J.; Bagyinka, C.; Hoffman, B. M.; Maroney, M. J. *J. Am. Chem. Soc.* **1993**, *115*, 5629–5635.
(43) Wang, S.; Lee, M. H.; Hausinger, R. P.; Clark, P. A.; Wilcox, D. E.; Scott, R. A. *Inorg. Chem.* **1994**, *33*, 1589–1593.
(44) Furenlid, L. R.; Renner, M. W.; Fajer, J. *J. Am. Chem. Soc.* **1990**, *112*, 8987–8989.
(45) Shiemke, A. K.; Shelnut, J. A.; Scott, R. A. *J. Biol. Chem.* **1989**, *264*, 11236–11245.
(46) Eidsness, M. K.; Sullivan, R. J.; Scott, R. A. In *The Bioinorganic Chemistry of Nickel*; Lancaster, J. R., Jr., Ed.; VCH: New York, 1988; pp 73–91.

Acknowledgment. This work was supported by a grant from the NIH (GM-38829, M.J.M.). Research carried out at the National Synchrotron Light Source, Brookhaven National Laboratory, is supported by the U.S. Department of Energy, Division of Materials Sciences and Division of Chemical Sciences (DOE Contract No. DE-AC02-76CH00016). We also thank the National Biostructures PRT (NIH-RR-01633) for beam-time allocations, technical assistance, and access to equipment. L.-F.W. and M.-A.M.-B. acknowledge the support of the CNRS and the Ministère de l'Enseignement Supérieur et de la Recherche.

Supporting Information Available: Tables of fits of K-edge EXAFS data (7 pages). Ordering information is given on any current masthead page.

IC980407T